Journal of Materials Chemistry B

PAPER

View Article Online
View Journal | View Issue

Cite this: J. Mater. Chem. B, 2014, 2, 4442

Recyclable enzyme mimic of cubic Fe_3O_4 nanoparticles loaded on graphene oxide-dispersed carbon nanotubes with enhanced peroxidase-like catalysis and electrocatalysis†

Hua Wang,*[a] Shuai Li,[a] Yanmei Si,[a] Zongzhao Sun,[a] Shuying Li[a] and Yuehe Lin*[bc]

Received 5th April 2014
Accepted 7th May 2014

DOI: 10.1039/c4tb00541d

www.rsc.org/MaterialsB

Fe_3O_4 nanoparticles as nanocatalysts may present peroxidase-like catalysis activities and high electrocatalysis if loaded on conductive carbon nanotube (CNT) supports; however, their catalysis performances in an aqueous system might still be challenged by the poor aqueous dispersion of hydrophobic carbon supports and/or low stability of loaded iron catalysts. In this work, amphiphilic graphene oxide nanosheets were employed as "surfactant" to disperse CNTs to create stable graphene oxide-dispersed CNT (GCNT) supports in water for covalently loading cubic Fe_3O_4 nanoparticles with improved distribution and binding efficiency. Compared with original Fe_3O_4 nanos and CNT-loaded Fe_3O_4 nanocomplex, the prepared GCNT–Fe_3O_4 nanocomposite could achieve higher aqueous stability and, especially, much stronger peroxidase-like catalysis and electrocatalysis to H_2O_2, presumably resulting from the synergetic effects of two conductive carbon supports and cubic Fe_3O_4 nanocatalysts effectively loaded. Colorimetric and direct electrochemical detections of H_2O_2 and glucose using the GCNT–Fe_3O_4 nanocomposite were conducted with high detection sensitivities, demonstrating the feasibility of practical sensing applications. Such a magnetically recyclable "enzyme mimic" may circumvent some disadvantages of natural protein enzymes and common inorganic catalysts, featuring the multi-functions of high peroxidase-like catalysis, strong electrocatalysis, magnetic separation/recyclability, environmental stability, and direct H_2O_2 electrochemistry.

1. Introduction

Enzymes have been widely applied as biological catalysts in environmental, industrial, medical, and biosensing fields.[1–3] However, there are certain disadvantages of natural enzymes, such as protein enzymes, regarding protease digestion, easy denaturation, and catalytic activity inhibition especially in some complex media (*i.e.*, wastewater). Moreover, natural enzyme-based electrochemical sensors can also be challenging as a result of the redox center of enzymes deep inside insulate protein shells, making electronic mediators/relays necessary.[4–7] Alternatively, increasing efforts have been contributed to development of inorganic catalysts that possess the catalysis capacities of natural enzymes but address some of their catalysis limitations.[8–19] In particular, the development of peroxidase-like nanocatalysts has attracted much attention.[13–18] Fe_3O_4 nanoparticles (Fe_3O_4 nanos), the most well-known example, have been established to possess intrinsic peroxidase-like catalysis activities through converting Fe^{2+}/Fe^{3+}.[13,17,18] Fe_3O_4 catalysts, however, may suffer from limited catalysis performance, low suspending stability, and poor metal oxide conductivity, especially for electrocatalysis applications. Accordingly, many conductive materials, typically as carbon nanotubes (CNTs), have been introduced as supports for Fe_3O_4 loading, owing to their high electric conductivity, large surface area, mechanical strength, and chemical inertness.[7,18,20–25] CNTs were mainly used to increase the electrocatalysis capacities of Fe_3O_4 nanocatalysts so as to achieve low-potential sensing of H_2O_2 or glucose[26] or their electromagnetic behaviour.[27] Meanwhile, CNT improvement of the intrinsic peroxidase-like catalysis of Fe_3O_4 nanocatalysts has received comparatively little attention. Some researchers have introduced CNTs to obtain enhanced catalysis of Fe_3O_4 nanocatalysts;[18] nevertheless, their catalysis performances and large-scale applications can still be challenged by the poor dispersion of hydrophobic carbon supports and low stability of iron catalysts mixed in an aqueous

[a]Shandong Province Key Laboratory of Life-Organic Analysis, School of Chemistry and Chemical Engineering, Qufu Normal University, Qufu City 273165, P.R. China. E-mail: huawangqfnu@126.com

[b]Pacific Norwest National Laboratory, Richland, WA 99352, USA. E-mail: yuehe.lin@wsu.edu; Fax: +01 509 371 6242; Tel: +01 509 371 6241

[c]School of Mechanical and Materials Engineering, Washington State University, Pullman, WA 99164, USA

† Electronic supplementary information (ESI) available: The kinetic characterization of peroxidase-like activities of GCNT–Fe_3O_4 nanocomposites comparing to HRP. See DOI: 10.1039/c4tb00541d

system. Therefore, improved spatial distribution and well-dispersion stability of CNT supports should be one of the key requirements to obtain further enhanced peroxidase-like catalysis and electrocatalysis of Fe_3O_4 nanocatalysts.

At present, two types of oxidation treatment[28] and surfactant addition[22] are normally used to improve the aqueous dispersion of hydrophobic CNTs, but with limited success. In recent years, graphene has received a great deal of attention in the materials science and biotechnology fields.[16,29–32] Reduced graphene oxide (GO) nanosheets have also been used to attach Fe_3O_4 nanos, achieving excellent electrocatalytic activities.[33] Particularly, GO nanosheets are amphiphilic with an edge-to-center distribution of hydrophilic and hydrophobic domains,[30] implying that they may serve as a very effective "surfactant" for CNTs to create stable colloidal dispersion in water.[30–32] In addition, it is well established that the catalysis activities of inorganic nanocatalysts could be shape- and size-dependent[34–37]—that is, cubic platinum nanoparticles have been demonstrated to show strong peroxidase-like catalysis.[36] In the present work, cube-shaped Fe_3O_4 nanos have been synthesized and further covalently bound onto the GO nanosheet-dispersed CNTs (GCNTs), aiming to develop a new kind of magnetic nanocatalyst with enhanced peroxidase-like catalysis and electrocatalysis performances towards extensive applications. Comparable investigations were carried out to demonstrate the improved support dispersion, high environmental stability, and especially enhanced peroxidase-like catalysis and electrocatalysis activities of the as-prepared GCNT–Fe_3O_4 nanocomposites by optical and electrochemical measurements, including the feasibility for recyclable sensing applications for H_2O_2 and glucose detection.

2. Experimental section

2.1. Materials and reagents

Multiple-walled CNTs functionalized with carboxyl groups were purchased from Carbon Solutions, Inc. (Riverside, CA). Graphene oxide nanosheets were obtained from Graphene Supermarket (USA). Glucose oxidase (GOD), glucose, human erythrocyte AChE, bovine serum albumin, Nafion (5.0%), *N*-(3-dimethylaminopropyl)-*N*-ethylcarbodiimide (EDC), *N*-hydroxysuccinimide (NHS), $FeCl_3$, sodium oleate, MES buffer, tetramethylammonium hydroxide (TMAH), and peroxidase colour substrate were the products of Sigma-Aldrich, including 3,3′,5,5′-tetramethylbenzidine (TMB), *o*-phenylenediamine (OPD), 3,3′-diaminobenzidine (DAB), *p*-aminophenol (PAP), and hydroquinone (HQ). Other reagents were of analytical reagent grade.

2.2. Synthesis of cubic Fe_3O_4 nanos

Cubic Fe_3O_4 nanos were synthesized by following the procedures of thermal decomposition of iron oleate complex.[37,38] Typically, $FeCl_3$ (5.0 mmol) and sodium oleate (15 mmol) were added to a mixture containing ethanol (10 ml), water (7.5 ml), and hexane (17.5 ml). The mixture was then refluxed at 60 °C for 4 h. After the organic reagents were separated and evaporated out, the resulting iron oleate was dissolved in an appropriate amount of 1-octadecene containing sodium oleate (2.5 mmol). The mixture was further heated to 300 °C for 40 min under nitrogen. The cooled solution was precipitated by 2-propanol, and then washed with hexane and ethanol. The precipitate of Fe_3O_4 nanos was subsequently resuspended in 1.0 M of TMAH as the stock suspension.

2.3. Preparation of and GOD modification of GCNT–Fe_3O_4 nanocomposite

The GCNTs were prepared with the mass ratio of GO nanosheets to CNTs at 1 : 10. An aliquot of 100 mg CNTs, which were treated to be derivatized with carboxyl groups, were ultrasonicated in 50 ml deionized water for 30 min, and then 10 mg GO solution was added to the CNT solution to be sonicated until a visually homogeneous dispersion was formed. The resulting GCNT mixture was sonicated for 16 h (cycles of 60 s on and 5 s off), and then centrifuged and washed to get GCNTs. Furthermore, the GCNT–Fe_3O_4 nanocomposite was synthesized by the EDC/NHS cross-linking chemistry. An aliquot of carboxyl group-derivatized GCNTs described above were re-dispersed in an MES buffer (pH 5.0) containing 100 mM EDC and 80 mM NHS to be stirred overnight at room temperature. The activated GCNTs were then separated and washed twice by centrifuge. Moreover, an aliquot of cubic Fe_3O_4 nanos of the desired amount in TMAH above was magnetically separated and washed three times. The yielding precipitate of amine-derivatized Fe_3O_4 nanos was then mixed with the activated GCNTs suspension for 3 h (pH 7.0), followed by magnetic separation and washing. The resulting GCNT–Fe_3O_4 nanocomposite was finally dispersed in 2-propanol at different concentrations. In addition, a CNT–Fe_3O_4 nanocomplex was prepared in the same manner except for the GO addition.

Thereafter, 1.0 mg of GCNT–Fe_3O_4 nanocatalysts was dispersed in 1.0 ml PBS containing 0.5% Triton X-100. GOD (10 mg) was added to an aliquot of GCNT–Fe_3O_4 suspension (1.0 mg ml^{-1}) pre-activated by EDC/NHS chemistry to be incubated overnight at 4 °C. Then the mixture was magnetically separated and washed twice. Subsequently, GOD-loaded GCNT–Fe_3O_4 nanocomposites were dispersed in PBS containing 0.5% Triton X-100 to be stored at 4 °C.

2.4. Colorimetric catalysis experiments

Colorimetric tests were performed to comparably examine the peroxidase-like catalysis activities among various suspensions (0.01 mg in 1.0 ml PBS, pH 4.5) of CNTs, GCNTs, Fe_3O_4 nanos, CNT–Fe_3O_4, and GCNT–Fe_3O_4 nanocatalysts, which were separately added to 0.15 ml TMB–H_2O_2 substrates. Moreover, the organic peroxidase substrates (2.0 mM) of TMB, DAB, OPD, PAP, and HQ were catalytically oxidized by mixing them with 4.0 mM H_2O_2 using the 0.01 mg ml^{-1} GCNT–Fe_3O_4 suspension to produce different colors of reaction products. In addition, colorimetric detection for glucose and H_2O_2 of different concentrations was conducted in an acetate buffer (0.2 M, pH 4.5) containing 4.0 mM TMB using GOD-loaded GCNT–Fe_3O_4 and GCNT–Fe_3O_4 nanocomposites (0.01 mg ml^{-1}), respectively. Moreover, the dynamics parameters (*i.e.*, K_m and V_{max}) of GCNT–Fe_3O_4 nanocomposites were measured in order to plot Michaelis–Menten curves with different concentrations of H_2O_2 and TMB.

2.5. Electrochemical catalysis experiments

Electrocatalytic investigations of the GCNT–Fe_3O_4-modified electrode for H_2O_2 were performed using the CHI 760 electrochemical analyzer (CH Instruments, Austin, TX). A three-electrode configuration (CH Instruments) consisting of a glassy carbon working electrode, an Ag/AgCl reference electrode, and a platinum counter electrode was employed. Herein, 5 μl of the respective suspension (0.010 mg in 1.0 ml 0.25% Nafion) of CNTs, GCNTs, Fe_3O_4 nanos, and GCNT–Fe_3O_4 nanocomposites were separately dropped onto the electrodes to be incubated overnight at 4 °C. Subsequently, 5 μl of 0.05% Nafion were added onto the electrodes and left for 1 h at room temperature.

Furthermore, cyclic voltammetry (CV) measurements of the resulting electrodes were conducted in a PBS solution containing the same H_2O_2 concentration. The direct electrochemical responses of the GCNT–Fe_3O_4-modified electrode to successive additions of H_2O_2 with a step of 1.0 mM were recorded under the same CV conditions. Moreover, glucose was electroanalyzed with the GOD–GCNT–Fe_3O_4-modified electrode. Herein, an appropriate amount of the GOD-labeled GCNT–Fe_3O_4 nanocatalysts was first dispersed in PBS buffer with 0.25% Nafion. An aliquot of 5.0 μl of the mixture was added onto the electrodes to be incubated overnight at 4 °C and washed twice. The amperometric responses to glucose with different concentrations for the resulting enzyme electrodes were recorded at an applied potential of −0.3 V.

3. Results and discussion

3.1. Synthesis and characterization of GCNT–Fe_3O_4 nanocomposite

Cube-shaped Fe_3O_4 nanos were synthesized by the thermal decomposition of iron oleate complex,[37,38] and stabilized in TMAH solution to be derivatized with amine groups.[38,39] The yielded Fe_3O_4 nanos were further separately coupled onto the carboxyl group-functionalized CNTs and the GCNTs (mass ratio of GO to CNTs being 1 : 10) by EDC/NHS cross-linking chemistry, resulting in GCNT–Fe_3O_4 nanocomposites. Fig. 1 shows the comparison of topological structures among different nanomaterials by transmission electron microscopy (TEM) imaging. Note that cubic Fe_3O_4 nanos (~13 nm in diameter) could largely be loaded onto CNTs and GCNTs to form the CNT–Fe_3O_4 (Fig. 1C) and GCNT–Fe_3O_4 (Fig. 1D), respectively. However, the latter may display much higher dispersion and suspension stability than the former, as is clearly shown in their solution photographs. Moreover, the TEM images show that Fe_3O_4 nanocatalysts were well distributed and aligned with desirable density on the GCNT–Fe_3O_4 nanocomposites (Fig. 1D, inset); in contrast, they were stacked and coagulated on the CNT–Fe_3O_4 nanocomplex. Clearly, the GCNT supports could enable better binding distribution and dispersion stability of Fe_3O_4 nanos on the nanocomposite, confirming the vital role of the GO "surfactant." The synergetic effects of carbon supports (high conductivity or electron transfer) and of cubic Fe_3O_4 nanos (intrinsic catalysis activity) were thereby expected to facilitate both enhanced peroxidase-like catalysis and electrocatalysis of GCNT–Fe_3O_4 nanocomposite for recyclable sensing applications.

3.2. Colorimetric investigations of peroxidase-like catalysis activities of GCNT–Fe_3O_4 nanocomposite

We first employed the peroxidase substrate of TMB–H_2O_2 to investigate the peroxidase-like catalysis activities of the obtained GCNT–Fe_3O_4 nanocatalysts (Fig. 2). Fig. 2A shows the comparison of colorimetric TMB–H_2O_2 reaction results among CNTs, GCNTs, Fe_3O_4 nanos, CNT–Fe_3O_4, and GCNT–Fe_3O_4. One can find that both CNTs and GCNTs may show a small amount of catalysis behaviour, which may result from the presence of

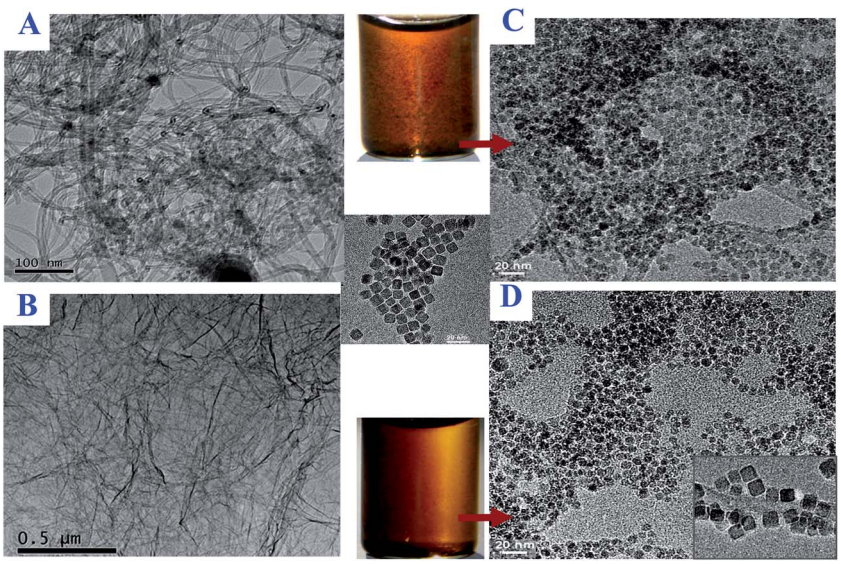

Fig. 1 Typical TEM images of (A) CNTs, (B) GO, (C) CNT–Fe_3O_4 nanocomposite, (D) GCNT–Fe_3O_4 nanocomposite (inset: partially amplified view of a nanocomposite), and free cubic Fe_3O_4 nanos (middle), including (middle, top and bottom) the photographs of the CNT–Fe_3O_4 and GCNT–Fe_3O_4 suspensions indicated.

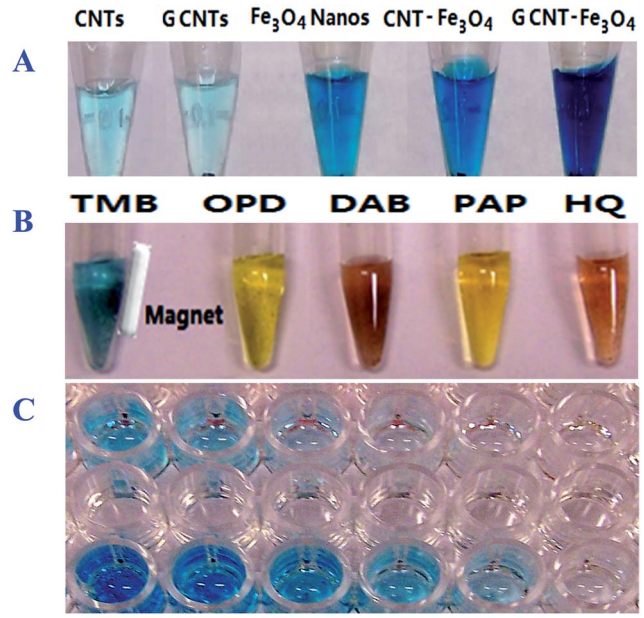

Fig. 2 Colorimetric comparison investigations of catalysis activities of GCNT–Fe_3O_4 nanocatalysts. (A) Comparison of catalytic activities for TMB–H_2O_2 reaction (5.0 mM TMB and 2.0 mM H_2O_2) among CNTs, GCNTs, Fe_3O_4 nanos, CNT–Fe_3O_4, and GCNT–Fe_3O_4 materials normalized with the same iron amount. (B) GCNT–Fe_3O_4-catalyzed H_2O_2 oxidization of various organic peroxidase substrates (2.0 mM) of TMB, OPD, DAB, PAP, and HQ. (C) Colorimetric detection of glucose (top row) and H_2O_2 (bottom row), ranging from 0.050 to 1.0 mM (from right to left) using GOD-loaded GCNT–Fe_3O_4 and pure GCNT–Fe_3O_4 nanocatalysts (0.010 mg ml^{-1}), respectively.

catalysis-active iron segments of CNTs,[18,23,40] and/or the intrinsic peroxidase-like catalytic activity of GO nanosheets.[16] But Fe_3O_4 nanos showed stronger catalysis than the commercially available CNTs or GCNTs in terms of color densities of TMB–H_2O_2 reaction products. More importantly, when Fe_3O_4 nanos were loaded on GCNTs, the resulting GCNT–Fe_3O_4 nanocomposites could show much higher catalysis activity than Fe_3O_4 nanos and carbon supports; furthermore, they could exhibit much stronger peroxidase-like catalysis than the CNT–Fe_3O_4, demonstrating the apparent difference in catalyst supports. Again, the use of GO "surfactant" could significantly improve the aqueous dispersion and stability of the supports to allow for better distribution and more effective loading of cubic Fe_3O_4 nanocatalysts, which may in turn facilitate greatly enhanced peroxidase-like catalysis activities of GCNT–Fe_3O_4 nanocomposites by faster conversion of Fe^{2+}/Fe^{3+}.[13]

In addition, the kinetic characterization of peroxidase-like activities of GCNT–Fe_3O_4 nanocomposites was carried out by plotting the typical Michaelis–Menten curves (Fig. S1, ESI†). According to the Lineweaver–Burk equation, the Michaelis constant (K_m) and the maximal reaction velocity (V_{max}) were obtained and shown in Table S1, ESI,† as compared with those of the natural enzyme, horseradish peroxidase (HRP), reported elsewhere.[13] It is found that the K_m value of the GCNT–Fe_3O_4 with a H_2O_2 substrate (2.52 mM) is a little lower than that of HRP (3.7 mM), showing that they could have compatible affinity to H_2O_2. But the GCNT–Fe_3O_4 presented much lower K_m with a TMB substrate (0.118 mM) than HRP (0.434 mM), indicating higher affinity to TMB was achieved for the GCNT–Fe_3O_4, presumably resulting from its carbon carriers with strong adsorption to TMB.

3.3. Colorimetric sensing applications of GCNT–Fe_3O_4 nanocomposite

The peroxidase-like catalysis activities of GCNT–Fe_3O_4 nanocatalysts were first examined *via* the H_2O_2-induced catalytic oxidation of some organic peroxidase substrates commonly used, including TMB, OPD, DAB, PAP, and HQ. Fig. 2B shows the photographs of the colorimetric reaction products. It was discovered that these originally colourless organic substrate solutions could be rapidly turned into various colours; for instance, the DAB solution presented a brown colour. Clearly, the GCNT–Fe_3O_4 enzyme mimic may display strong catalysis degradation of typical organic peroxidase substrates. Note that when a magnetic stirring bar was applied to the side of the tube after color reactions, magnetic nanocatalysts could be effectively collected from the substrate media, as exemplified in the TMB tube in Fig. 2B. Therefore, the strong magnetism of GCNT–Fe_3O_4 nanocatalysts could additionally enable the inorganic nanocatalysts to be recovered or recycled after usage, indicating the possibility of extensive applications in the field of environmental chemistry. For example, they may be tailored for the magnet-aided separation and recyclable catalysis degradation or removal of organic toxicants such as phenols[18] in wastewater treatments.

Furthermore, TMB–H_2O_2 substrate reactions catalyzed by the developed GCNT–Fe_3O_4 nanocomposite were found to be pH-dependent, which was colorimetrically tested by changing the pH values from pH 0.50 to pH 14 (data not shown). The optimal pH value of the reaction was found to be ~pH 4.5, as determined by the fastest reaction of blue substrates. Additionally, when the GCNT–Fe_3O_4 catalysts were placed at 90 °C for 1 h or stored at room temperature for 6 months, no significant change was observed in their catalysis performance for TMB–H_2O_2 reactions (data not shown). The results indicate that the inorganic enzyme mimic can display high thermal and long-term storage stabilities. Subsequently, the feasibility of catalysis applications for colorimetric H_2O_2 and glucose detection was probed using GCNT–Fe_3O_4 and GOD–GCNT–Fe_3O_4 nanocatalysts, respectively (Fig. 2C). A proportional change of colour densities for TMB chromogens was obtained for H_2O_2 and glucose, both with linear concentrations ranging from 0.050 to 1.0 mM, by separately plotting the absorbance values *versus* H_2O_2 and glucose concentrations (data not shown), indicating the potential for sensitive colorimetric detection of H_2O_2 and glucose.

3.4. Electrochemical investigations of electrocatalysis activities of GCNT–Fe_3O_4 nanocomposite

The GCNT–Fe_3O_4 nanocatalysts were coated onto the electrodes to conduct direct electrocatalysis to H_2O_2 reduction, in comparison with the electrodes modified separately with CNTs,

GCNTs, Fe_3O_4 nanos, and CNT–Fe_3O_4. Fig. 3 illustrates the typical CVs of these electrodes, in which significantly different changes in H_2O_2 response currents were observed upon adding 3.0 mM H_2O_2. Interestingly, the current response of the CNT-modified electrode was higher than that of the Fe_3O_4 nano-modified electrode, but was lower than that of the electrodes modified with GCNTs or CNT–Fe_3O_4. Compared with CNTs, semiconductive Fe_3O_4 nanos might be packed more tightly on the electrode, leading to lower electron transportation—although they had high peroxidase-like catalysis activity in the previous experiments. As for the GCNT-modified electrode, relatively high electrocatalysis to H_2O_2 was observed, presumably resulting from the intrinsic electrocatalysis activities of CNTs and/or GO, as evidenced elsewhere.[16,22,33,41–43] From Fig. 3, one can observe that the H_2O_2 reduction response of the GCNT–Fe_3O_4-modified electrode was ~2.5 times higher than that of the electrode with Fe_3O_4 nanos or GCNT alone. Also, it could exhibit much larger responses to H_2O_2 than the CNT–Fe_3O_4-modified one. Accordingly, stronger electrocatalysis to H_2O_2 was verified for the GCNT–Fe_3O_4 electrode, including higher electron transfer capacities, presumably benefiting from the high electrocatalysis of carbon supports,[16,18,22,23,33] and the aforementioned intrinsic peroxidase-like catalysis of Fe_3O_4 nanos.

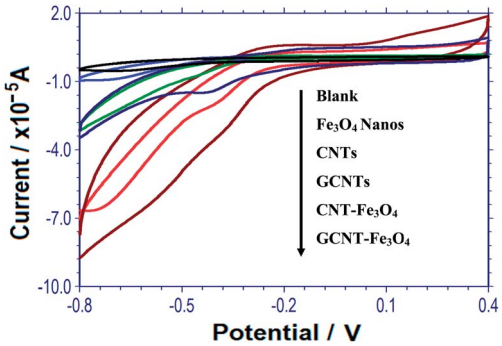

Fig. 3 Comparison of direct voltammetric responses to H_2O_2 (3.0 mM) among the electrodes separately modified with GCNTs, CNTs, Fe_3O_4 nanos, and the CNT–Fe_3O_4 and GCNT–Fe_3O_4 nanocomposites, scanning from −0.80 to 0.40 V at a scan rate of 0.10 V s^{-1}.

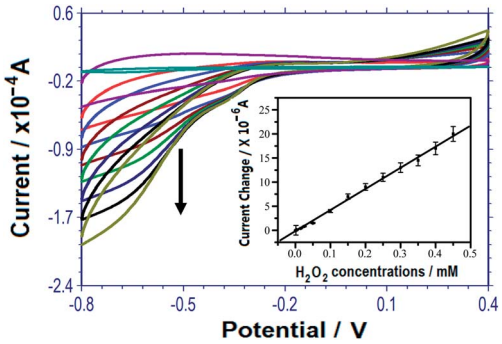

Fig. 4 Direct voltammetric responses of the GCNT–Fe_3O_4-modified electrode to successive 1.0 mM step additions of H_2O_2. Inset: the calibration curve of amperometric responses to H_2O_2 with different concentrations linearly ranging from 0.01 to 0.50 mM.

3.5. Electrochemical-sensing applications of GCNT–Fe_3O_4 nanocomposites

Fig. 4 manifests the direct voltammetric responses of the GCNT–Fe_3O_4-modified electrode to successive additions of H_2O_2. It was observed that the CV responses could increase proportionally with increasing H_2O_2 levels linearly ranging from 0.010 to 0.50 mM. Of note, the interference of other electroactive substances such as ascorbic acid and uric acid can be largely excluded if H_2O_2 was detected at such a low overpotential.[22,33,44]

Moreover, the electrochemical detections of glucose by the electrode modified with GCNT–Fe_3O_4-loaded GOD were conducted (Fig. 5). Herein, GOD was covalently loaded onto the GCNT–Fe_3O_4-modified electrodes forming the enzyme sensor for glucose analysis through amperometric detection of liberated H_2O_2. A typical current–time response curve was obtained for the enzyme sensor to successive additions of glucose at an applied potential of −0.3 V (Fig. 5A). Note that the current responses could increase with increasing glucose concentrations, in which the steady-state signals were reached in less than ~10 s.

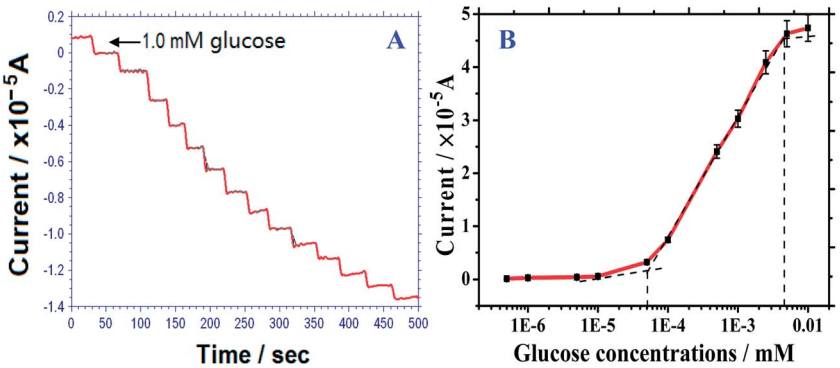

Fig. 5 (A) Typical current–time responses of the GCNT–Fe_3O_4-modified electrode combined with GOD to successive addition of glucose with a 1.0 mM step, measured at an applied potential of −0.3 V. (B) Steady-state calibration curve of amperometric responses to glucose with various concentrations ranging from 0.050 to 5.0 mM.

Fig. 5B describes the calibration curve of the GOD sensor for glucose samples with various concentrations. Linear concentrations of glucose were achieved ranging from 0.050 to 5.0 mM, with a detection limit of 0.022 mM. Accordingly, the developed electrode could exhibit much better performances of sensing to glucose than the electrodes modified with CNT-loaded GOD, as previously documented.[22]

4. Conclusions

In this study, cubic Fe_3O_4 nanos were successfully synthesized and covalently bound onto the GO nanosheet-dispersed CNTs supports leading to GCNT–Fe_3O_4 nanocomposites with enhanced peroxidase-like catalysis and electrocatalysis activities. On the one hand, the introduction of GO nanosheets could significantly improve the aqueous dispersion of hydrophobic CNT supports to allow for more effective and stable loadings of Fe_3O_4 nanocatalysts. On the other hand, the synergetic effects of two carbon supports of high conductivity and electron-transfer capability, and cubic Fe_3O_4 nanos of intrinsic catalysis activity, could facilitate greatly improved peroxidase-like catalysis and electrocatalysis activities. Compared with natural enzymes or even common iron-based nanocatalysts like the CNT–Fe_3O_4 nanocomplex, the resulting GCNT–Fe_3O_4 nanocomposites could possess advantages of: (1) strong peroxidise-like catalysis to catalyze the H_2O_2-induced oxidization of typical peroxidase substrates so as to enable sensitive H_2O_2-based detections; (2) high electron-transferring and electrocatalysis capabilities, to allow for direct electrochemistry to H_2O_2 at a low over-potential; (3) unique magnet-aided separation and organic catalysis degradation abilities to facilitate recyclable catalytic detoxification or removal of organic pollutants (*i.e.*, phenols) in the environment and in wastewater; and (4) high environmental stability against high temperature and long-term storage. The outstanding catalysis performances of the GCNT–Fe_3O_4 nanocatalysts have been subsequently demonstrated by colorimetric and direct electrochemical sensing of H_2O_2 and glucose with high detection sensitivity. This recyclable enzyme mimic holds great promise of intensive applications in recyclable biological catalysis, magnetic separation, toxicant removal or degradation, and enzyme-based sensing analysis fields. Significantly, such a synthesis protocol using an "artificial enzyme" may open a new door towards multifunctional catalyst design by dispersing magnetic nanocatalysts onto two high-surface-area carbon supports.

Acknowledgements

This work is supported by the National Institutes of Health, Counter ACT Program, through the National Institute of Neurological Disorders and Stroke of the United States (NS058161-01), the National Natural Science Foundation of China (21375075), and the Taishan Scholar Foundation of Shandong Province, P.R. China.

The contents of this publication are solely the responsibility of the authors and do not necessarily represent the official views of the Federal Government. PNNL is operated by Battelle for DOE under Contract DE-AC05-76RL01830.

Notes and references

1 E. Torres, I. Bustos-Jaimes and S. Le Borgne, *Appl. Catal., B*, 2003, **46**, 1–15.
2 A. Mueller, *Mini-Rev. Med. Chem.*, 2005, **5**, 231–239.
3 N. Q. Ran, L. S. Zhao, Z. M. Chen and J. H. Tao, *Green Chem.*, 2008, **10**, 361–372.
4 A. E. G. Cass, G. Davis, G. D. Francis, H. A. O. Hill, W. J. Aston, I. J. Higgins, E. V. Plotkin, L. D. L. Scott and A. P. F. Turner, *Anal. Chem.*, 1984, **56**, 667–671.
5 G. Arai, K. Shoji and I. Yasumori, *J. Electroanal. Chem.*, 2006, **591**, 1–6.
6 J. Wang, *Analyst*, 2005, **130**, 421–426.
7 J. Wang, *Chem. Rev.*, 2008, **108**, 814–825.
8 V. Nanda and R. L. Koder, *Nat. Chem.*, 2010, **2**, 15–24.
9 A. J. Kirby, *Angew. Chem., Int. Ed.*, 1996, **35**, 707–724.
10 R. Breslow, X. J. Zhang and Y. Huang, *J. Am. Chem. Soc.*, 1997, **119**, 4535–4536.
11 L. Fruk and C. M. Niemeyer, *Angew. Chem., Int. Ed.*, 2005, **44**, 2603–2606.
12 A. Asati, S. Santra, C. Kaittanis, S. Nath and J. M. Perez, *Angew. Chem., Int. Ed.*, 2009, **48**, 2308–2312.
13 L. Z. Gao, J. Zhuang, L. Nie, J. B. Zhang, Y. Zhang, N. Gu, T. H. Wang, J. Feng, D. L. Yang, S. Perrett and X. Yan, *Nat. Nanotechnol.*, 2007, **2**, 577–583.
14 W. C. Ellis, C. T. Tran, M. A. Denardo, A. Fischer, A. D. Ryabov and T. J. Collins, *J. Am. Chem. Soc.*, 2009, **131**, 18052–18053.
15 B. Meunier, in *Biomimetic Oxidations Catalyzed by Transition Metal Complexes*, Imperial College Press, Covent Garden, 2000, pp. 171–214.
16 Y. J. Song, K. G. Qu, C. Zhao, J. S. Ren and X. G. Qu, *Adv. Mater.*, 2010, **22**, 1–5.
17 H. Wei and E. Wang, *Anal. Chem.*, 2008, **80**, 2250–2254.
18 X. L. Zuo, C. Peng, Q. Huang, S. P. Song, L. H. Wang, D. Li and C. H. Fan, *Nano Res.*, 2009, **2**, 617–623.
19 A. T. Bell, *Science.*, 2003, **299**, 1688–1691.
20 J. Wang and Y. H. Lin, *TrAC, Trends Anal. Chem.*, 2008, **27**, 619–626.
21 R. H. Baughman, A. A. Zakhidov and W. A. de Heer, *Science.*, 2002, **297**, 787–792.
22 J. Wang, M. Musameh and Y. H. Lin, *J. Am. Chem. Soc.*, 2003, **125**, 2408–2409.
23 B. Sljukic, C. E. Banks and R. G. Compton, *Nano Lett.*, 2006, **6**, 1556–1558.
24 H. Yan, H. J. Zhou, P. Yu, L. Su and L. Q. Mao, *Adv. Mater.*, 2008, **20**, 2899–2906.
25 R. Laocharoensuk, J. Burdick and J. Wang, *ACS Nano*, 2008, **2**, 1069–1075.
26 S. W. Qu, J. Wang, J. L. Kong, P. Y. Yang and G. Chen, *Talanta*, 2007, **71**, 1096–1102.
27 L. Zhang, Q. Q. Ni, T. Natsuki and Y. Q. Fu, *Appl. Surf. Sci.*, 2009, **255**, 8676–8681.

28 M. S. Saha and A. Kundu, *J. Power Sources*, 2010, **195**, 6255–6261.
29 X. L. Li, X. R. Wang, L. Zhang, S. Lee and H. J. Dai, *Science.*, 2008, **319**, 1229–1232.
30 L. J. Cote, J. Kim, V. C. Tung, J. Luo, F. Kim and J. Huang, *Pure Appl. Chem.*, 2011, **83**, 95–110.
31 J. Ma, L. Zhou, C. Li, J. H. Yang, T. Meng, H. M. Zhou, M. X. Yang, F. Yu and J. H. Chen, *J. Power Sources*, 2014, **247**, 999–1004.
32 L. L. Tian, M. J. Meziani, F. S. Lu, C. Kong, Y. L. Cao, T. J. Thorne and Y. P. Sun, *ACS Appl. Mater. Interfaces*, 2010, **2**, 3217–3222.
33 H. Teymourian, A. Salimi and S. Khezrian, *Biosens. Bioelectron.*, 2013, **49**, 1–8.
34 T. S. Ahmadi, Z. L. Wang, T. C. Green, A. Henglein and M. A. El-Sayed, *Science.*, 1996, **272**, 1924–1926.
35 F. F. Peng, Y. Zhang and N. Gu, *Chin. Chem. Lett.*, 2008, **19**, 730–733.
36 M. Ma, Y. Zhang and N. Gu, *Colloids Surf., A*, 2011, **373**, 6–10.
37 M. V. Kovalenko, M. I. Bodnarchuk, R. T. Lechner, G. Hesser, F. Schaffler and W. Heiss, *J. Am. Chem. Soc.*, 2007, **129**, 6352–6353.
38 J. Jiang, H. W. Gu, H. L. Shao, E. Devlin, G. C. Papaefthymiou and J. Y. Ying, *Adv. Mater.*, 2008, **20**, 4403–4407.
39 L. E. Euliss, S. G. Grancharov, S. O'Brien, T. J. Deming, G. D. Stucky, C. B. Murray and G. A. Held, *Nano Lett.*, 2003, **3**, 1489–1493.
40 J. Kruusma, N. Mould, K. Jurkschat, A. Crossley and C. E. Banks, *Electrochem. Commun.*, 2007, **9**, 2330–2333.
41 C. E. Banks, T. J. Davies, G. G. Wildgoose and R. G. Compton, *Chem. Commun.*, 2005, **7**, 829–841.
42 K. P. Gong, S. Chakrabarti and L. M. Dai, *Angew. Chem., Int. Ed.*, 2008, **47**, 5446–5450.
43 I. Dumitrescu, P. R. Unwin and J. V. Macpherson, *Chem. Commun.*, 2009, 6886–6901.
44 K. Yamamoto, G. Shi, T. S. Zhou, F. Xu, J. M. Xu, T. Kato, J. Y. Jin and L. Jin, *Analyst*, 2003, **128**, 249–254.